Cellulose
https://doi.org/10.1007/s10570-024-06197-w

ORIGINAL RESEARCH

Ozone-loaded bacterial cellulose hydrogel: a sustainable antimicrobial solution for stone cleaning

Erica Sonaglia · Emily Schifano · Simone Augello · Mohammad Sharbaf · Fabrizio Marra · Arianna Montanari · Luciana Dini · Maria Sabrina Sarto · Daniela Uccelletti · Maria Laura Santarelli

Received: 4 April 2024 / Accepted: 25 September 2024

Abstract The use of biocide-loaded hydrogels has recently been exploited for cleaning the biological attacks of cultural heritage and architectural stone materials. However, considering the drawbacks of traditional biocides, and the high costs of synthetic polymers, growing research for innovative and sustainable solutions are taking place. The aim of this work is to explore a bacterial cellulose (BC) hydrogel functionalized with ozone as a renewable, biodegradable, and easy-to-use antimicrobial remedy for stone biodeterioration. The BC microstructure was characterized by Field Emission-Scanning Electron Microscopy observation and high crystallinity was detected by X-ray diffraction analysis. Ozonated BC (OBC) hydrogels were tested against selected biodeteriogenic microorganisms in water suspension abolishing their viability, with its complete suppression after a 10-min and a 24-h treatment with OBC, for bacterial and fungal spores, respectively. Furthermore, the OBC was assessed on contaminated marble, brick, and biocalcarenitic stone specimens for simulating in situ conditions. A 100% reduction of microbial viability after a 24-h treatment was obtained. Successively, the shelf-life of the hydrogel and the antimicrobial activity were also evaluated after 30 days, demonstrating a subsequent cleaning efficiency along time. This research highlights the potential of the new ozonated BC hydrogel as a green and highly effective antimicrobial treatment, with advantages in sustainability.

Keywords Bio-hydrogel · Antimicrobial · Ozone · Superficial cleaning

Erica Sonaglia and Emily Schifano have contributed equally to this work.

Supplementary Information The online version contains supplementary material available at https://doi.org/10.1007/s10570-024-06197-w.

E. Sonaglia · M. Sharbaf · M. L. Santarelli (✉)
Department of Chemical Engineering Materials and Environment, Sapienza University of Rome, Via Eudossiana 18, 00184 Rome, Italy
e-mail: marialaura.santarelli@uniroma1.it

E. Schifano · S. Augello · A. Montanari · L. Dini · D. Uccelletti (✉)
Department of Biology and Biotechnologies "C. Darwin", Sapienza University of Rome, P.Le Aldo Moro 5, 00185 Rome, Italy
e-mail: daniela.uccelletti@uniroma1.it

F. Marra · M. S. Sarto
Department of Astronautical, Electrical and Energy Engineering, Sapienza University of Rome, Via Eudossiana 18, 00184 Rome, Italy

F. Marra · L. Dini · M. S. Sarto · D. Uccelletti
Research Center for Nanotechnology Applied to Engineering, Sapienza University of Rome, P.Le Aldo Moro 5, 00185 Rome, Italy

Published online: 02 October 2024

Introduction

Biodeterioration of stone materials is a significant concern in their maintenance, as this degradation can have detrimental effects on historical monuments, sculptures, and, generally, architectural structures made of stone (Gaylarde and Little 2022). It refers to the processes through which living organisms, such as microorganisms, algae, lichens, and plants, contribute to the degradation of surfaces, by secreting acids and producing extracellular polymers that facilitate stone decay (Negi and Sarethy 2019). Indeed, microbial colonization can lead to several detrimental processes, including biogenic acid corrosion, physical damage due to root growth, and pigments-derived staining produced by microorganisms (Liu et al. 2020). Environmental conditions, such as temperature, humidity, and pollution levels, play a pivotal role in influencing the rate and extent of biodeterioration (Zhang et al. 2019). Microbial colonization of stone is influenced by these environmental factors and petrologic properties of the stone itself, especially its chemical composition, types of minerals present, as well as roughness, porosity and water permeability (Liu et al. 2018; Schifano et al. 2020). Notably, different types of stone materials exhibit varying susceptibilities to biodeterioration; for instance, limestone is more vulnerable than granite due to its higher porosity.

Various strategies have been employed to mitigate biodeterioration, such as cleaning and protecting stone surfaces, controlling environmental factors, and applying biocides or consolidants to inhibit microbial growth (Kakakhel et al. 2019; Romani et al. 2022).

Non-destructive testing methods, among which infrared spectroscopy and microbial DNA analysis, are increasingly used to assess the extent of biodeterioration without causing further harm to the stone (Cappitelli et al. 2007; Cutler et al. 2012; Grazzini et al. 2020; Salvatici et al. 2023). On the other hand, biodeterioration treating methods also involve substrate damages and other disadvantages. For instance, the removal of biological growth through physical or chemical cleaning methods, such as scrubbing, pressure washing, or using biocides, can be abrasive, damaging delicate stone surfaces, not providing long-term protection (Warscheid and Braams 2000). Moreover, application of chemicals as traditional biocides to inhibit microbial growth on stone surfaces may have environmental and health concerns, short-term effectiveness, can harm non-target organisms and select resistant biodeteriogens (Kakakhel et al. 2019).

Consequently, innovative eco-friendly methods are required, offering environmental sustainability, long-term efficacy, preservation of aesthetics, reduced health risks, and minimal harm to non-target organisms. In recent years, there has been a significant increase in the use of phytochemicals, such as plant extracts or essential oils, due to their strong inhibitory effects as natural and environmentally friendly biocides (Rugnini et al. 2020; Favero-Longo et al. 2022). These complex mixtures of natural compounds are associated with various mechanisms of action against microorganisms, including the enhanced permeability of the cytoplasmic membrane, resulting in its integrity loss, and the inhibition or activation of enzymatic reactions (Palla et al. 2020). On the other hand, the use of essential oils is related to some disadvantages. Indeed, essential oils are generally volatile, resulting in less persistence compared to other chemical antimicrobial agents and may require frequent applications to maintain effectiveness in biodeterioration control. Some of them can cause allergic reactions or other unwanted side effects in sensitive individuals. Moreover, their action can be selective and limited to specific bacterial or fungal strains and can be sensitive to factors like oxidation and light, which can compromise their stability over time. Finally, high-quality essential oils can be expensive to produce and purchase (Cappitelli et al. 2020). Over the past decade, the search for new cleaning methods has led to the development of hydrogels, three-dimensional hydrophilic cross-linked, water-inflated polymer networks that can retain a significant amount of water without dissolving (Ahmed 2015). When employed in the mitigation of stone biodeterioration, hydrogels demonstrated the release of inhibitors or biocides in a controlled manner, effectively limiting the growth of microorganisms responsible for deterioration (Gabriele et al. 2022).

In addition, hydrogels can reduce solvent evaporation, can efficiently adhere to vertical surfaces, prevent solvent dripping, and allow extended treatment times, reducing the amount of biocide needed and increasing treatment efficacy (De France et al. 2020; Boccalon et al. 2021). Since the introduction of hydrogels in the cultural heritage field, synthetic formulations have shown effective performance

(Domingues et al. 2013; Baglioni et al. 2019). However, the drawbacks associated with the use of synthetic polymers, such as the lack of renewability and biodegradability and their high costs, highlighted the need for innovative and sustainable solutions. For this reason, it would be desirable to formulate hydrogels composed of renewable and non-toxic materials. Indeed, biopolymers represent an eco-friendly and safe alternative to synthetic polymers, offering environmental friendliness, and biocompatibility (Caruso et al. 2023).

To develop new eco-friendly remedies against the stone biodeterioration, in this study a bacterial cellulose (BC) water hydrogel was enriched by ozone and its antimicrobial activity was evaluated against different biodeteriogenic microorganisms.

Materials and methods

Bacterial cellulose (BC) hydrogel characterization

The bacterial cellulose (BC) pellicle derived from kombucha was generously supplied in the wet state from an Italian brewer located at Meda (MB). This material will be referred to as hydrogel, since it is constituted by a polymeric network swollen with water. Indeed, this material differs from cryogel that is obtained by freeze-thawing cycles and from aerogel which retains a gaseous phase in the polymeric network. Samples of approximately 10 cm × 10 cm × 0.5 cm were treated three times with an aqueous solution of 0.5 M sodium hydroxide (NaOH, Merck, Darmstadt, Germany) at 85 °C for 1 h. Afterwards the BC was washed with H_2O_{dd} until neutral pH and stored in H_2O_{dd} at 4 °C until further use.

Samples of BC hydrogel were freeze-dried using a Lyovapor L-200 instrument (Buchi, Flawil, Switzerland) and the microstructure was studied using a Zeiss Auriga 405 Field Emission-Scanning Electron Microscope (FE-SEM) (Zeiss, Oberkochen, Germany). Samples were analysed at different accelerating voltages (varying between 1.0 and 1.2 keV). Fibril and aggregate diameter distributions were evaluated using ImageJ 1.53 k Java 1.8.0_172 software for 100 measurements each on SEM images of sample surfaces.

The BC crystallinity was studied on freeze-dried samples of approximately 2 cm × 2 cm by X-ray diffraction analysis using a D8 Advance diffractometer (Bruker AXS Gmbh, Germany). The diffractometer operates with Mo–Ka radiation (λ = 0.7093 Å, 40 keV, 35 mA) in Bragg–Brentano geometry. Angular scanning was carried out between 3.3° and 29.98° with a step of 0.01°. To minimise the background, a home-made "fork type" sample stage which uses a metal support with two rods and a Mylar film as the base was employed. X-ray diffraction patterns were converted in the $Cu_{K\alpha 1}$ (λ = 1.5418 Å) wavelength. The crystallinity index (CrI) (%) was calculated according to Segal et al. (1959) (Eq. 1), where I_{200} is the maximum intensity of the (2 0 0) lattice diffraction and I_{am} is the diffraction intensity related to the amorphous region at 2θ ~ 18°.

$$CrI(\%) = \frac{\left(I_{200} - I_{am}\right)}{I_{200}} \times 100 \quad (1)$$

The interplanar spacing (d) was calculated by means of Bragg's law (Eq. 2), where n (integer) is the order of reflection, λ is the wavelength of the incident X-rays and θ is the angle of incidence.

$$n\lambda = 2dsin(\theta) \quad (2)$$

The average crystallite size (L) (nm) along the cell plane related to the main peak was calculated using the Scherrer equation (Eq. 3), where K_s is a shape factor constant in the range 0.8–1.2 (typically equal to 0.89), λ is the X-ray wavelength, τ is the peak full width in radians at half maximum (FWHM), θ is the Bragg angle.

$$L = \frac{K_s\lambda}{(cos\theta)\tau} \quad (3)$$

The abundance of cellulose I_α and I_β allomorphs was estimated as reported by Wada and co-workers (Wada and Okano 2001) (Eq. 4), where d_1 (nm) is the d-spacing of $(100)_{I\alpha}$ and $(1\underline{1}0)_{I\beta}$ planes; d_2 (nm) is the d-spacing of $(010)_{I\alpha}$ and $(110)_{I\beta}$ planes. Z value is > 0 for I_α-rich type cellulose and < 0 for I_β-rich type cellulose.

$$Z = 1693_{d1} - 902_{d2} - 549 \quad (4)$$

To study the viscoelastic properties of BC, rheological measurements were carried out using a MCR302 Rheometer (Anton Paar GmbH, Graz, Austria). The analysis was conducted according to

Numata et al. (2019) (Numata et al. 2019). Briefly, BC samples were cut into circular pieces with a diameter of 25 mm and held on the 25-mm flat parallel plates of the rotational rheometer. The gap was controlled by a normal force of 0.2 N. Every specimen underwent a dynamic strain sweep, ranging from 0.001 to 100% and frequency of 1 Hz, to determine the linear viscoelastic range. An optimal strain of 0.01% was identified and consequently employed for the frequency sweeps. The measurements were carried out at room temperature, with an angular frequency in the range of 0.1–100 rad/s.

Uniaxial elongation studies were performed on the BC hydrogel according to Pacelli et al. (2018) (Pacelli et al. 2018). Briefly, the hydrogels having a rectangular shape of 45 mm × 15 mm have been fixed in an Instron 5982 (Instron, Milan, Italy). The samples were elongated at room temperature at the rate of 1 mm/min until the breaking point. From the stress–strain curve, the maximum percentage of elongation ε, the maximum yield stress σ, and the elastic modulus E were derived.

Ozonation process of BC hydrogels and ozone concentration analysis

BC hydrogels were loaded with ozone by using an OZONIS STERIL 250 series ozone generator (Sepra S.R.L., Italy) with a capacity of 5.2 mmol/h of ozone with a constant gas flow rate of 1.5 l/min. Ozonated BC (OBC) hydrogels with 0.223 mmol/g (OBC-L, low), 0.381 mmol/g (OBC-M, medium), and 0.531 mmol/g (OBC-H, high) ozone concentrations were obtained by varying ozonation times and water volumes. Specifically, OBC-L was obtained after 6 h of ozonation in 60 mL of H_2O_{dd} while the OBC-M was produced after 24 h in the same volume of H_2O_{dd}. The same time was instead applied in 20 mL of H_2O_{dd} to generate the OBC-H samples. As an alternative control the OBC-H samples were washed 2 times with H_2O_{dd}, until the ozone was discharged (OBC-W). Ozone concentration in the OBC hydrogels was estimated for each batch by calculating the mmol of ozone loaded in one sample (dry weight) as follows. After ozonation, the samples were immersed in 10 ml of H_2O_{dd} and left at 4 °C in a rotating wheel. After 20 min, an aliquot was collected and ozone concentration in water (mmol/L) was determined photometrically using an Hach DR1900 spectrophotometer with LCK310 kit (Hach Lange, Spain), based on the colorimetric method with N,N-diethyl-p-phenylenediamine (DPD). Water was subsequently exchanged, and the procedure was repeated until no ozone was further detected (ozone < 0.001 mmol/L). The moles of total ozone loaded in the BC hydrogel samples were estimated based on its concentrations in all the exchanged water aliquots and the total volume of water used. The OBC hydrogels were stored at 4 °C until further analysis.

Characterization of ozonated BC hydrogels

To evaluate the potential interaction of ozone with cellulose, chemical structures of OBC-L, OBC-M, OBC-H and the pristine BC hydrogels were analyzed by Attenuated Total Reflectance-Fourier Transform Infrared Spectroscopy (ATR-FTIR). Spectra were acquired on freeze-dried samples using a Vertex 70 spectrometer (Bruker Optics, Gmbh, Ettlingen, Germany) equipped with a single reflection Diamond ATR cell, a standard MIR source (HeNe) and a room temperature DTGS detector. The spectra were recorded with 64 scans in the mid-infrared range (400–4000 cm^{-1}) at a resolution of 4 cm^{-1}.

The water holding capacity (WHC) of OBC-M, OBC-H and the pristine BC hydrogels was calculated according to the formula reported by Ul-Islam et al. (2012) (Ul-Islam et al. 2012) (Eq. 5), where M_{wet} is the mass of the water-swollen sample, and M_{dry} is the mass of the dried sample at 60 °C until no weight change is detected. Prior to weighing the wet sample, the excess of surface water was removed by tapping with a tissue. Measurements were conducted in quadruplicate.

$$WHC = \frac{M_{wet} - M_{dry}}{M_{dry}} \quad (5)$$

The microstructure analysis, the XRD analysis as well as the rheological characterization of OBC-L, OBC-M and OBC-H, were performed as described before. To assess the effect of ozonation on cellulose mechanical properties, uniaxial elongation studies were performed on oven-dried OBC and pristine BC hydrogels at 60 °C. Samples having a rectangular shape of 45 mm × 15 mm have been fixed in an Instron 5982 (Instron, Milan, Italy) with a 500N load

cell and elongated at room temperature at the rate of 2 mm/min until the breaking point.

Microbial strains and growth conditions

The bacterial strains utilized in this study included the gram-positive *Arthrobacter aurescens*, *Arthrobacter agilis*, *Kocuria rosea*, and the gram-negative *Achromobacter xylosoxidans* species. They were cultivated in Luria–Bertani (LB) broth under aerobic conditions at 30 °C. The fungal strains employed belonged to *Aspergillus jensenii*, *Cladosporium cladosporioides*, and *Alternaria alternata* species, and were cultured at 30 °C in Sabouraud medium. All bacterial and fungal species had been previously isolated in Motya (Sicily, Italy).

Antimicrobial activity evaluation

To assess the antibacterial activity, 0.2 mL of cells with a concentration of 2×10^6 cells/mL derived from overnight cultures of *A. xylosoxidans*, *A. aurescens*, *A. agilis* or *K. rosea* was incubated at room temperature in the presence of the three ozonated BC hydrogels. At specified intervals of 1, 10, 20, and 60 min of treatment, aliquots from the various samples were subjected to a series of dilutions to ensure an appropriate concentration for plating. The dilutions were prepared using sterile H_2O_{dd} to maintain the integrity of the samples. Subsequently, 100 µL of each diluted sample was spread onto LB (Luria–Bertani) agar plates using a sterile spreader to ensure uniform distribution. The plates were incubated at 28 °C for 18–24 h to allow for bacterial growth. Following incubation, the number of colony-forming units (CFU) on each plate was determined by counting the distinct colonies. Each colony represents a viable bacterial cell from the original sample. The CFU count was then used to calculate the bacterial concentration in the original sample, considering the dilution factor. All experiments were performed in triplicate. Bacterial samples incubated with pristine BC hydrogel served as control. The experiments were conducted in triplicate and repeated a minimum of three times. To evaluate possible membrane damages of bacteria treated with OBC-H hydrogel, the LIVE/DEAD BacLight (Thermo Fisher Scientific) was utilized according to the manufacturer's instructions. The kit is composed of two nucleic acid binding fluorescent dyes: SYTO 9 and propidium iodide (PI). With an appropriate mixture of SYTO 9 and PI stains, bacteria with intact cell membranes stain fluorescent green, scored as viable ones; and bacteria with injured membranes stain fluorescent red. Images were acquired with a Zeiss Axiovert 25 fluorescent microscope equipped with a 100X oil-immersion objective. The antisporogenic activity was assessed using 0.03 mL of a spores' suspension with a concentration of 1×10^4 spores/mL of *C. cladosporioides*, *A. jensenii*, or *A. alternata*. Each spore suspension was incubated in the presence of ozonated BC hydrogels. At intervals of 6 and 24 h, aliquots from each sample were diluted and subsequently plated on Sabouraud agar plates. After incubation at 30 °C, the spores' ability to germinate was determined by CFU method. Spore samples incubated with a pristine BC hydrogel served as control. The experiments were conducted in triplicate and repeated a minimum of three times.

Antimicrobial activity assay on stone specimens

For these experiments, specimens of marble, brick, and biocalcarenitic stone measuring $5\times5\times2$ cm were sterilized under UV light. For antibacterial assessment, 1 cm × 1 cm areas were chosen on each specimen, and 8×10^8 cells suspension of *A. aurescens* was applied to each area. After overnight incubation at room temperature, the contaminated areas were treated with OBC-M or OBC-H hydrogels, while the pristine BC hydrogel was taken as a control. The hydrogels were covered with sterile plastic film to minimize water evaporation and were peeled off using tweezers after 2, 6, and 8 h. To assess the antisporogenic activity, marble and biocalcarenitic stone specimens were used. For each lithotype, a 1×10^4 spores' suspension of *A. jensenii*, *A. alternata* or *C. cladosporoides* in YPD medium was spotted on the selected area. After a three-day incubation at 30 °C, the mycelium that originated on the stone surfaces was treated by applying OBC-M or OBC-H hydrogels, while the pristine BC hydrogel was taken as a control. The hydrogels were covered with sterile plastic film to minimize water evaporation and were peeled off by tweezers after 6 and 24 h. The determination of bacterial and fungal survival was performed as reported in Santo et al. (2023) (Santo et al. 2023). The experiments were conducted in triplicate and repeated at least three times.

Evaluation of OBC hydrogel residues on treated stone

The possible presence of cellulosic residues on stone surface after the cleaning treatment was evaluated by μ-Raman analysis using a Senterra spectrometer (Bruker Optics, Gmbh, Ettlingen, Germany), equipped with a CW diode-pumped solid-state laser emitting at 532 nm. Analysis was conducted on a selected area of a marble specimen before and after a 24 h-treatment with the OBC-H hydrogel. The spectral resolution was 9 cm^{-1} and time of acquisition and number of scans were selected for reducing the fluorescence interferences. Five spectra were acquired on random spots of the selected area. A Raman spectrum of the sample dried at 60 °C was acquired as a reference.

Analysis of OBC hydrogel reusability on stone

To assess the potential reuse of the ozonated BC hydrogel, a marble specimen was used in an antimicrobial test. The specimen was sterilized under UV light and an 8×10^7 cells suspension of *A. aurescens* species was applied to selected areas. After overnight incubation at room temperature, one area was treated with OBC-H hydrogel, which was then covered with sterile plastic film to minimize water evaporation. After 2 h, the OBC hydrogel was peeled off by tweezers and immediately placed on another area for an additional 2 h. After each treatment, treated and control areas were carefully scraped and the CFU determined as reported in Santo et al. (2023) (Santo et al. 2023). The experiment was conducted in triplicate and repeated at least three times.

Shelf-life of OBC hydrogel

The antimicrobial activity of OBC-H samples stored in their ozonated batch water at 4 °C were assessed after 1, 5, 15 and 30 days. Antimicrobial activity was evaluated on *A. xylosoxidans* and *A. aurescens* bacterial species and on *A. jensenii* spores as previously described. Results were expressed as a percentage of activity relative to the fresh ozonated hydrogel. The experiments were conducted in triplicate and repeated a minimum of three times.

Results and discussion

Pristine BC characterization

The microstructure of the BC sample used in this study was determined by FE-SEM analysis. A network of cellulose fibrils, which are individual structural units forming aggregates, was identified. Specifically, the analysis of the sample surface (Fig. 1 a, b) and cross-sectional area (Fig. 1c) show an open structure with high and randomly oriented porosity. The percent distributions of diameters show the most frequent values are in the range 40–45 nm and 80–90 nm for fibrils and aggregates, respectively (Fig. 1 d, e). The results are in accordance with BC description reported in previous studies (Hu et al. 2014; Gao et al. 2016).

The BC crystallinity was investigated by XRD analysis. The diffractogram showed three peaks at approximately 2θ of 14, 17 and 23 (Fig. 2a). The diffraction pattern can be assigned to a type I cellulose found in native celluloses (Atalla and VanderHart 1984; French 2014). The peaks are assigned to the Iα and Iβ allomorphs, having Miller indices of (100), (010) and (110), and (1$\underline{1}$0), (110) and (200), respectively. Indeed, the I_α and I_β crystalline forms, respectively assigned to triclinic and monoclinic systems, are both present in the type I cellulose (Atalla and VanderHart 1984). The Z index introduced by Wada and Okano (2001) estimated the abundance of the two crystalline forms, as reported in the materials and methods section (Wada and Okano 2001). The Z positive value (19.5) indicates the prevalence of the Iα allomorph. The Segal crystallinity index (Cr.I.)(Segal et al. 1959) was evaluated equal to 94.0%, showing a high ratio between crystalline and amorphous phases, and the crystallite size calculated for the main peak at 2θ of 23 was 5.81 nm. The results are in accordance with BC diffraction data obtained by other studies (Wada and Okano 2001; Fawcett et al. 2013; Tsouko et al. 2015; Vasconcelos et al. 2017). Frequency sweeps, performed by rotational rheometer MCR302, on BC samples describe the behavior as a function of time, where for high frequencies fast motion is simulated over short times, while at low frequencies slow motion is simulated over long times or at rest. In this measurement, the storage modulus G', which represents the elastic part of viscoelastic behaviour, and the loss modulus G'', which

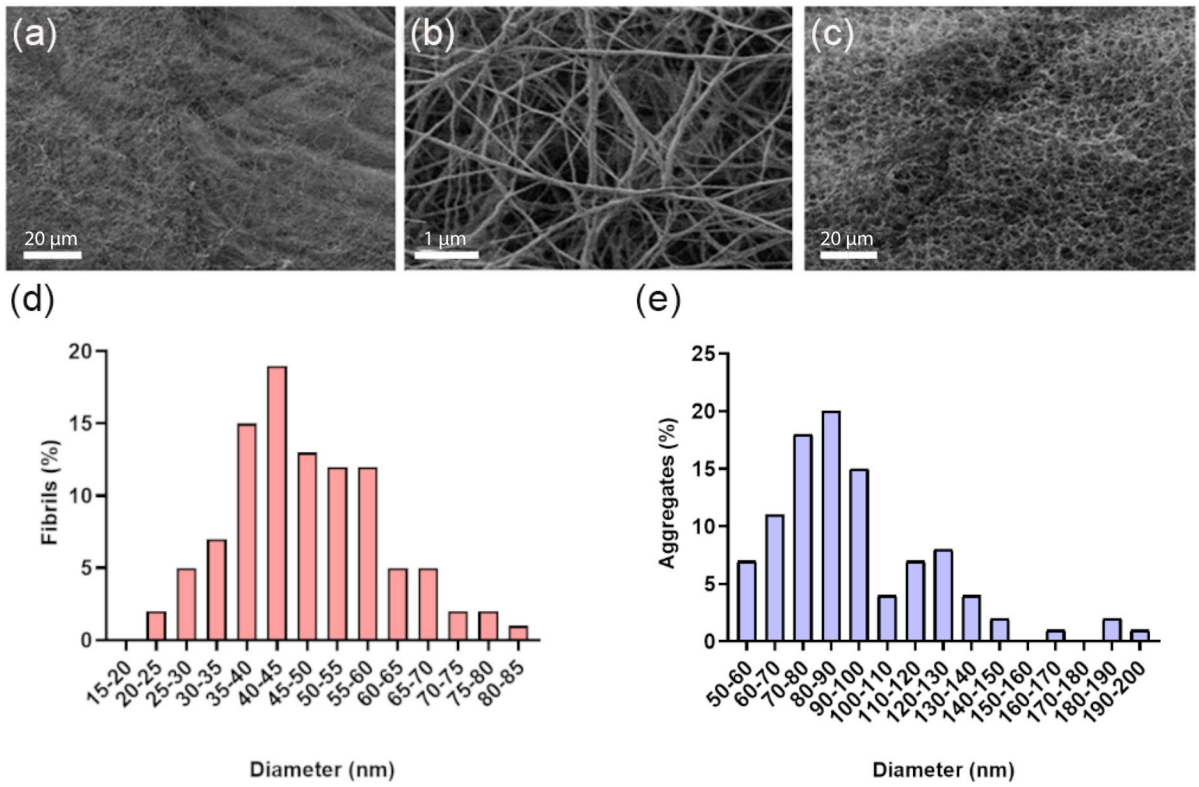

Fig. 1 Microstructural analysis of the BC hydrogel. **a** SEM micrograph on sample surface at 2kX magnification; **b** SEM micrograph on sample surface at 50kX magnification; **c** SEM micrograph on the cross-section at 2kX magnification; **d** Percent distribution of fibril diameters; **e** Percent distribution of aggregates diameters

characterizes the viscous part of viscoelastic behaviour, are measured. Figure 2b shows the trends of G' and G'' as a function of angular frequency, throughout the frequency range G' > G''. This behaviour indicates that the elastic response is predominant over the viscous response as also demonstrated in (Numata et al. 2019). This behaviour classifies BC as a self-supporting hydrogel (Orlando et al. 2020). In addition, the modulus G' exhibits a linear and nearly constant trend throughout the angular frequency range. The highlighted behaviour indicates that the cellulose network is not destabilized as the angular frequency increases, presenting high stability as the value of G' is strongly influenced by the intertwining of the fibrils (Chen et al. 2018). The BC mechanical properties were investigated by tensile testing. The stress (MPa)–strain (%) plot (Fig. 2c) displays a viscoelastic behaviour. The maximum percentage of elongation ε resulted in 15,5 ± 5,6%, the maximum yield stress σ is 18,4 ± 1,1 MPa and the elastic modulus E is 1,5 ± 0,6 MPa. The prevalent elastic behaviour, in accordance with the rheological results, is associated with the stretching of fibrils. The yield point and minor plastic deformation are related to the subsequent tearing and breaking of fibrils. The results are in accordance with other studies (Chen et al. 2018; Skvortsova et al. 2019).

Antimicrobial activity of ozonated BC hydrogels

Ozonated BC (OBC) hydrogels with various ozone concentrations were produced by employing different ozonation durations and volumes of water. The resulting samples are designated as OBC-L, OBC-M, and OBC-H, with ozone concentrations of 0.223 mmol/g, 0.381 mmol/g, and 0.531 mmol/g, respectively. Initially, to assess the OBCs antibacterial efficacy, a colony-forming unit (CFU) counting analysis was conducted in a liquid assay using various microbial species. Following a 10-min

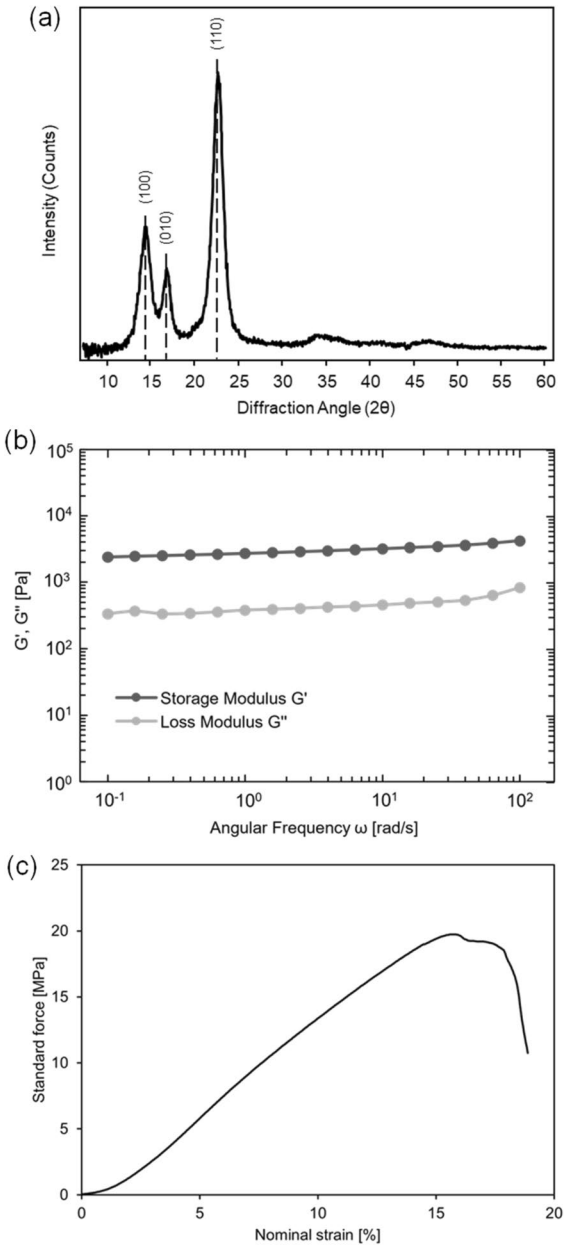

Fig. 2 Characterization of the BC hydrogel. **a** X-ray diffraction profile. Broken vertical lines indicate the positions of the main diffraction peaks, corresponding Miller indices of Cellulose Iα are indicated. **b** Viscoelastic behaviour studied by frequency sweep. **c** Representative stress (MPa)—strain (%) curve generated during tensile testing

treatment with OBC-M and OBC-H hydrogels, the mortality of *A. aurescens* exceeded 98%. Notably, OBC-H treatment resulted in a 60% cell mortality after just one minute. In contrast, OBC-L caused a 40% cell mortality after a 20-min treatment (Fig. 3a). Similar trends were observed in tests involving *A. agilis* and *K. rosea* species (data not shown). For *A. xylosoxidans*, treatment with OBC-H produced a 90% mortality after only one minute, reaching complete suppression of viability after 10 min (Fig. 3b). The same level of suppression was achieved with OBC-M after 20 min, while a 5% survival rate was observed after 1 h of treatment with OBC-L.

To evaluate a plausible mode of action of OBC hydrogels, the Live/Dead BacLight viability assay was used for analyzing if a bacterial cell membrane disruption occurred during the treatment. Indeed, while SYTO-9 penetrates and fluoresces green within all cells, the propidium iodide (red fluorescence) only penetrates within those with a compromised cell membrane. As shown in Fig. 3c, A.*aurescens* cells treated with OBC-H are stained with SYTO-9 and only few cells are stained with propidium iodide Instead, when the cells were treated with OBC-H the staining with propidium iodide was observed indicating that the ozonization affect the envelope of the cells. Indeed, the differences in antimicrobial efficacy observed among various bacterial species can be attributed to variations in bacterial cell wall composition, as *A. aurescens* is representative of gram-positives (alongside *A. agilis* and *K. rosea*), while *A. xylosoxidans* belongs to gram-negatives. However, the bacterial and fungal strains utilized in this study are established biodeteriogenic microorganisms, isolated from stone materials in various studies (Qi-Wang et al. 2011; Ettenauer et al. 2014; Tescari et al. 2018; Trovão et al. 2019).

Next, the anti-sporogenic effect against three fungal species was evaluated by assessing the germination ability of spores by the CFU counting method after treatment with various OBC hydrogels in a liquid assay. Specifically, for *A. jensenii*, a mortality rate exceeding 95% was evident as early as 6 h post-treatment with OCB-H hydrogel (Fig. 3d), reaching approximately 90% after 24 h. In the case of OCB-M treatment, a modest reduction in *A. jensenii* viability was observed at 6 h, decreasing to approximately 50% after 24 h. Conversely, treatment with the OBC-L sample showed no discernible effect on spore germination. Similar trends were observed for *A. alternata* and *C. cladosporioides* samples (Fig. 3e and f). In particular, the antibacterial effects of OCB-H are

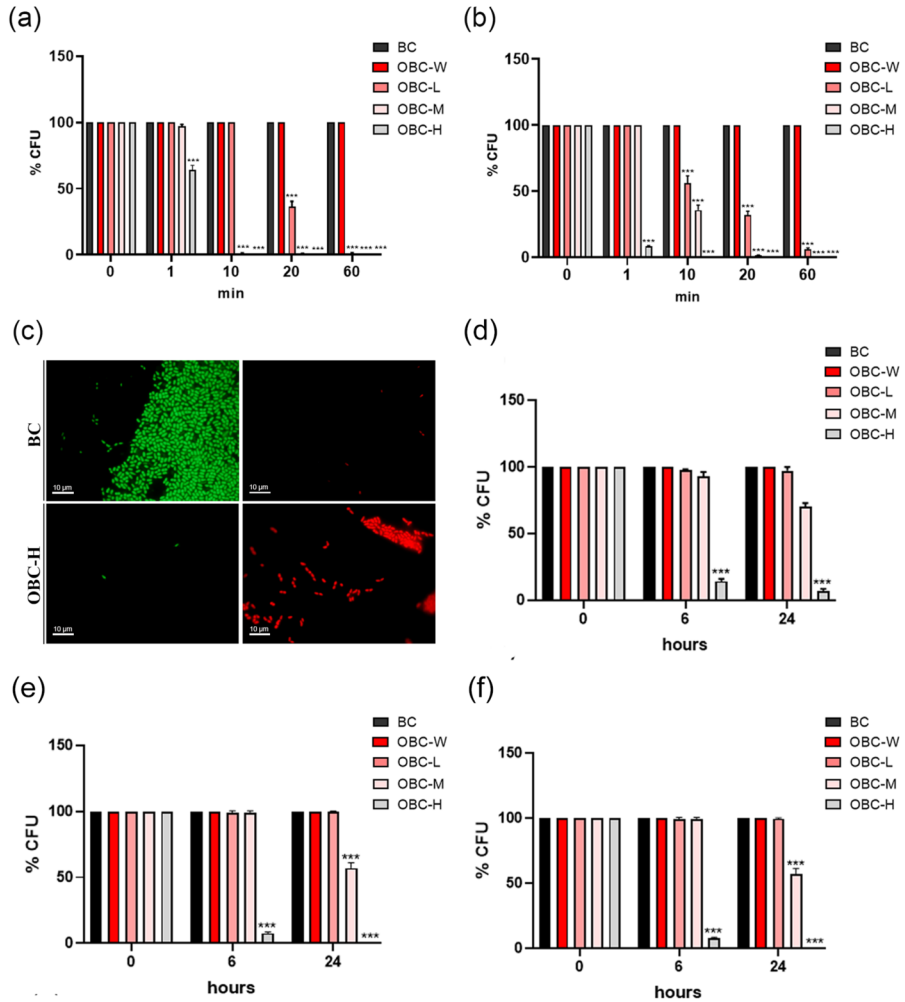

Fig. 3 Impact of OBC hydrogels on bacterial and fungal viability. *A. aurescens* (**a**) and *A. xylosoxidans* (**b**) were subjected to treatment with BC (control), OBC-W, OCB-L, OCB-M and OCB-H for different times, as indicated. Bacterial survival was evaluated using colony-forming unit (CFU) counting analysis. Data are presented as mean ± SD. Statistical significance was determined employing a one-way ANOVA analysis with the Bonferroni post-test (***$p < 0.001$ compared to the BC sample). In **c** *A. aurescens* cells exposed to Live/Dead stains after incubation with BC or OBC-H hydrogels. On the left SYTO-9 staining and, on the right, the propidium iodide staining. The germination capability of fungal spores assessed after treatment with OBC-W, OCB-L, OCB-M and OCB-H in a liquid assay **d**–**f**. BC treatment was taken as control. CFU counting was performed for *A. jensenii* (**d**), *A. alternata* (**e**) and *C. cladosporioides* (**f**) after different treatment times. Data are presented as mean ± SD. Statistical analysis was carried out using a one-way ANOVA with the Bonferroni post-test (***$p < 0.001$ compared to the BC sample)

even more efficient, reaching approximately 100% after 24 h for the two fungal species.

Among the hydrogels tested, OBC-H has emerged as the most promising candidate due to its antimicrobial properties. Literature reports various antimicrobial strategies, encompassing both conventional and innovative biocides, aimed at effectively reducing microbial presence on surfaces. Among these methods are the application of preventive antimicrobial agents, such as ZnO-nanorods (Zn-NRs), graphene nanoplatelets decorated with Zn-NRs and silver nanoparticles (AgNP) in superficial coatings of stone (Carrillo-González et al. 2016; Schifano et al. 2020).

Recently, essential oils (EOs) have gained significant attention as natural biocides for the restoration of

cultural heritage, serving as an alternative to chemical agents (Ranaldi et al. 2022). Nevertheless, their utilization on a larger scale is disadvantaged by factors such as production costs and a need of information regarding efficacy at low doses, treatment durability, and potential interactions with material substrates (Fidanza and Caneva 2019; Lo Schiavo et al. 2020; Romani et al. 2022).

Characterization of OBC hydrogels

The microstructure of OBC hydrogels was investigated by FE-SEM analysis. The OBC-H microstructure is shown in Fig. 4, where similar characteristics to the pristine BC properties are identified (Fig. 4 a, b, c). Indeed, the dimensional analysis does not show variation in the dimensions of fibrils and fibril aggregates, presenting the most frequent diameters in the range of 40–45 nm for fibrils and 80–90 nm for fibril aggregates (Fig. 4 d, e), as in pristine BC. Similar results were obtained for OBC-L and OBC-M samples (data not shown). Accordingly, the ozonation did not significantly affect the microstructure of the OBC hydrogels.

Frequency sweeps on OBC hydrogels were used to determine their viscoelastic behavior (Fig. 5a). Like pristine BC, all samples showed a storage modulus (G') greater than the loss modulus (G'') across the frequency range, indicating that the elastic response is dominant. Additionally, the storage modulus (G') remained linear and nearly constant throughout the angular frequency range for all samples, demonstrating that the ozonated cellulose network remains stable even at higher frequencies. Furthermore, an increase in the elastic modulus of the systems can be observed with the higher content of ozone (Fig. 5b).

The ATR-FTIR spectroscopy was employed to assess the effect of ozonation on the chemical structures of OBC-L, OBC-M and OBC-H samples. The infrared spectra of OBC-L, OBC-M, OBC-H and

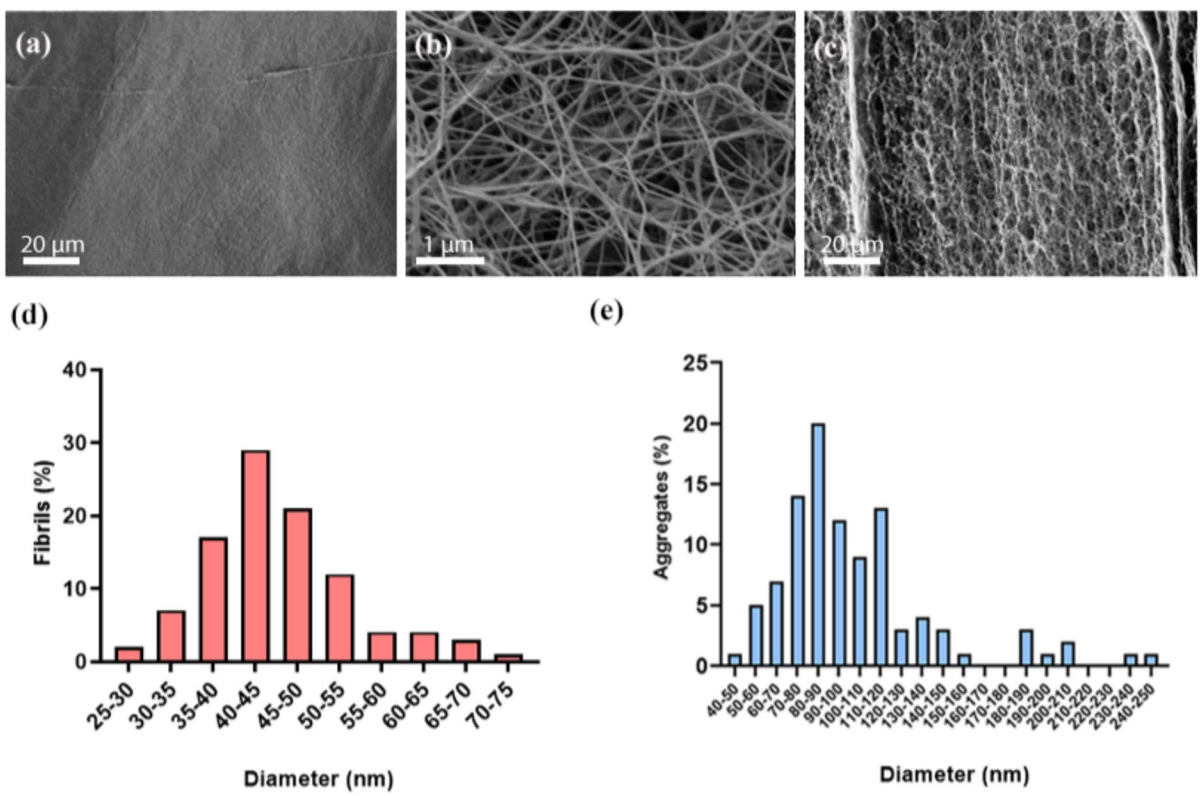

Fig. 4 Microstructural analysis of the OBC-H hydrogel. **a** SEM micrograph on sample surface at 2kX magnification; **b** SEM micrograph on sample surface at 50kX magnification; **c** SEM micrograph on the cross-section at 2kX magnification; **d** Percent distribution of fibril diameters; **e** Percent distribution of aggregates diameters

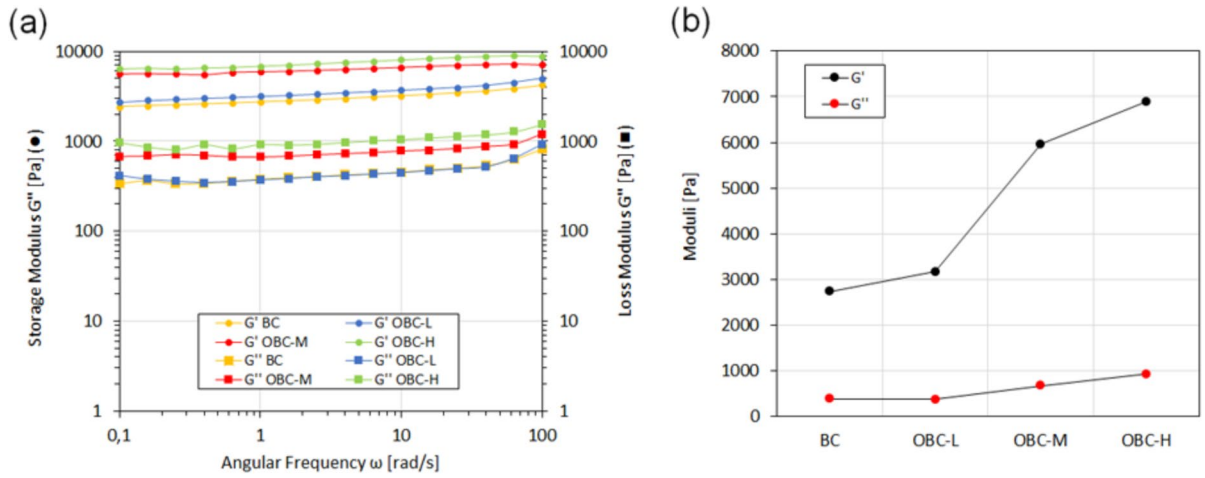

Fig. 5 Rheological characterization of OBC-L, OBC-M, OBC-H and BC hydrogels. **a** Viscoelastic behaviour analyzed by frequency sweep; **b** Storage (G') and loss (G'') moduli values taken at $\omega = 1$ rad/s from frequency sweep tests

the pristine BC exhibit the characteristic absorption of pure cellulose as compared in Fig. 6. A new signal at 1706 cm^{-1} in the spectra of all ozonated BC hydrogels has been observed, not present in pristine BC. Specifically, this signal is associated with the presence of carbonyl groups, more evident in OBC-H, due a partly weak oxidation of the BC cellulose, in agreement with literature reports (Chirat and Lachenal 1994; Costa et al. 2016; Tripathi et al. 2020).

The estimated WHC of the pristine BC hydrogel is 100.8 ± 3.9, comparable with the value for OBC-M (100.9 ± 6.2), instead the WHC is higher for OBC-H

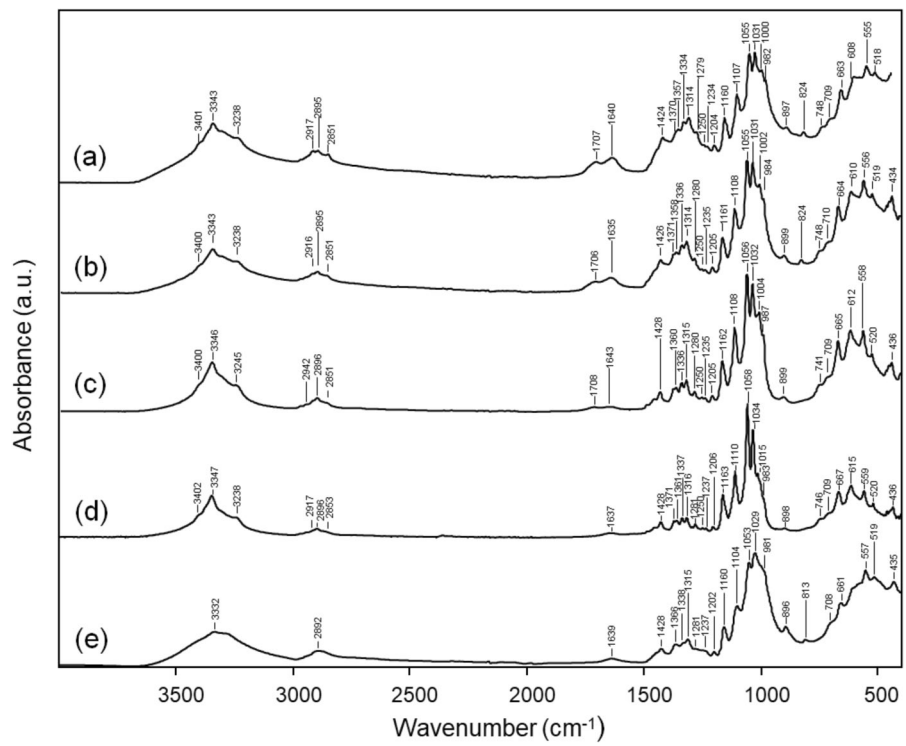

Fig. 6 Investigation by ATR-FTIR spectroscopy of the influence of ozonation on the chemical structure of BC hydrogel. Infrared spectra of OBC-H (**a**), OBC-M (**b**), OBC-L (**c**), pristine BC (**d**) hydrogels and pure cellulose (Sigma Aldrich CAS No. 9004–34-6) (**e**)

(152.6 ± 13.5). Considering that the WHC is related to BC network porosity, fibril aggregation, and superficial area (Ul-Islam et al. 2012; Paximada et al. 2016), the ozonation does not significantly affect the OBC-M hydrogel. Instead, an increase in WHC of OBC-H is observed in accordance with the more evident presence of carbonyl groups observed by the FTIR spectra, attested also for other oxidized bacterial celluloses (Lai et al. 2013; Mohammadkazemi et al. 2019). This behavior is also in agreement with the higher elastic modulus of the OBC-H, which results in a greater swelling of the network structure.

The XRD analysis was performed on OBC-L, OBC-M, and OBC-H samples to evaluate possible changes in BC crystallinity due to ozonation. Similarly to pristine BC, the diffractograms showed the peaks typical of type I cellulose (Fig. 7a). Also in these samples, the presence of the Iα allomorph is indicated by the positive Z index values (28.0, 10.4, and 6.9 for OBC-L, OBC-M, and OBC-H, respectively). A slight reduction in the Cr. I. was assessed with respect to the BC (91.1%, 90.2%, and 89.1% for OBC-L, OBC-M, and OBC-H, respectively). This behavior is also observed in other studies of oxidized bacterial cellulose (Vasconcelos et al. 2020; Yang et al. 2021). Furthermore, the analysis revealed a variation in the height of the 100 peak relative to the 110 and 010 peaks in the samples. The pristine BC (pattern d in Fig. 7a or Fig. 2a) exhibited minimal preferred orientation when compared to the ideal pattern for randomly oriented Iα reported in French (2014). In contrast, both OBC-L and OBC-H samples, as well as the OBC-M, displayed a preferred orientation involving a rotation about the c-axis, favoring the 100 plane as also mentioned in French (2014). The ozonation process and/or lyophilization of OBC samples may promote the observed alignment along the fibril axis. This effect has been identified by various authors as 'uniplanar orientation' in bacterial cellulose (Takai et al. 1975; Cai and Kim 2010; Chen et al. 2011). The changes in orientation highlighted by the XRD analysis do not appear to largely impact the microstructure of the hydrogel, as revealed by SEM analysis, although slight modifications could not be excluded. To evaluate if ozonated BC has a different tensile strength with respect to pristine BC, dried OBC samples were subjected to tensile testing. As reported in Fig. 7b the profile of the two samples

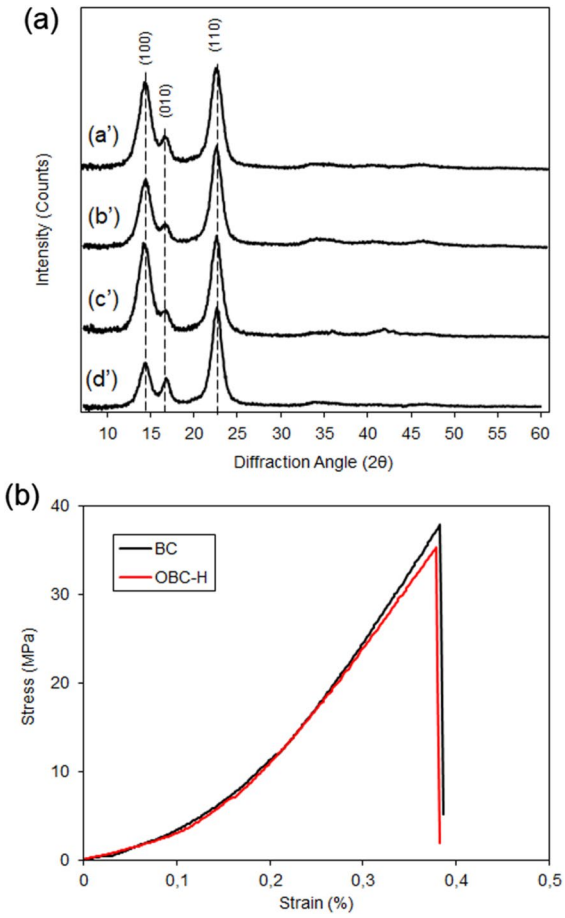

Fig. 7 Characterization of the OBC hydrogels. **a** X-ray diffraction profile of OBC-H (**a'**), OBC-M (**b'**), OBC-L (**c'**), pristine BC (**d'**). Broken vertical lines indicate the positions of the main diffraction peaks, corresponding Miller indices of Cellulose Iα are indicated. **b** Representative stress (MPa)—strain (%) curve generated during tensile testing of the dried BC and OBC-H samples

is almost identical. Similar results were also obtained for OBC-L and OBC-M (data not shown).

To determine if the antimicrobial action of OBC hydrogel is due to the ozonated water that swelled the hydrogel or it is due to the ozonated part of the cellulose, the OBC-H has been dried and its antimicrobial properties were tested. Indeed, the activity of the dried OBC-H hydrogel was studied through inhibition halo measurement against *A. aurescens*, showing any activities (Fig. S1). According to the results, BC hydrogel can be thus identified as a carrier for ozone-dissolved water.

The shelf-life of the OBC-H hydrogel was evaluated by studying the antimicrobial activity against *A. aurescens*, *A. xylosoxidans* and *A. jensenii* spores in liquid assays up to 30 days from production (Fig. 8).

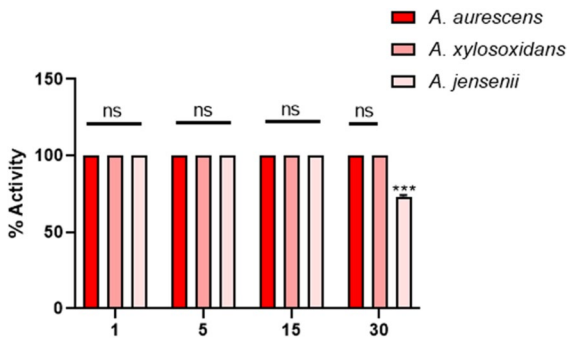

Fig. 8 Evaluation of the shelf-life of OBC-H hydrogel through the viability of *A. aurescens*, *A. xylosoxidans* and *A. jensenii*. Samples were stored in ozonated batch water at 4 °C for 1, 5, 15, and 30 days and then tested on bacterial and spore suspensions. Microorganisms' viability was determined through CFU counting analysis and results are reported as percentages of the relative activity related to the fresh ozonated hydrogels. Statistical significance was determined using a one-way ANOVA analysis with the Bonferroni post-test (ns indicating no significance; ***$p < 0.001$ compared to the control)

For all the investigated period, the sample exhibited a 100% of activity against the bacterial species compared to the freshly produced OBC-H sample, demonstrating that the antibacterial activity is maintained. Instead, the activity against the fungal spores shows a 30% reduction after a 30-day storage period. This behaviour is attributed to the higher ozone concentration required against fungal spores compared to bacteria.

Laboratory simulation experiments on stones

After the evaluation in a liquid assay, the antibacterial activities of ozonated BC hydrogels were assessed on different lithotypes, employing the representative bacterium *A. aurescens* isolate (Fig. 9). In all the specimens tested, OBC-H treatment successfully resulted in almost 100% mortality within just 2 h. The OBC-M sample on marble and brick specimens showed a high degree of mortality similarly to OBC-H application, for all the time analysed. On the contrary, the OBC-M on biocalcarenitic stone resulted in a significant reduction in cell viability, surpassing 98% only after 8 h of treatment. Promising results were also achieved when testing the spore germination capability on

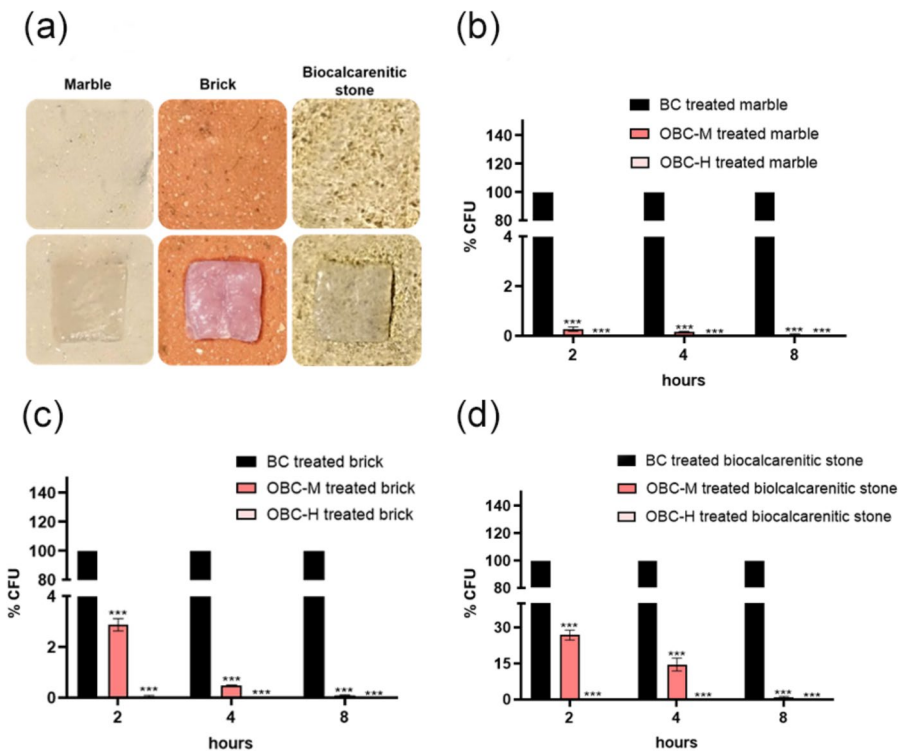

Fig. 9 Laboratory simulation experiment with the representative bacterium *A. aurescens*. Photographs of the employed lithotypes without (upper) and with (lower) OBC hydrogel application (**a**). Cell viability following treatment with OBC hydrogels for marble (**b**), brick (**c**), and biocalcarenitic stone (**d**) specimens, evaluated through CFU counting. Statistical analysis was conducted using a one-way ANOVA with the Bonferroni post-test (***$p < 0.001$ compared to BC sample)

biocalcarenite stone and marble, highlighting an antifungal activity of the OBC-H membrane exceeding 95% compared to the untreated control (Fig. 10).

In conclusion, after testing the antimicrobial efficacy on various lithotypes, OBC-H emerged as the most effective and promising candidate. This could potentially serve as a viable alternative to current biodeteriogen removal techniques in use, which, however, come with several disadvantages. Initially, mechanical removal methods were widely employed. Despite some advantages, these techniques may cause damage to the substrate. High-pressure water blasting, for instance, can push microorganisms deep into the heritage material (Cappitelli et al. 2020). Moreover, when microorganisms grow endolithically, penetrating pores, fissures, and cracks, mechanical removal becomes challenging. Residues in the form of single viable cells or entire colonies then become a source for rapid substrate recolonization. While natural biocides have shown success, there are drawbacks to using chemicals of natural origin, such as oils and plant extracts. The composition of these substances can vary significantly based on factors like harvesting season, geographical location, and other agronomic considerations (Nezhadali et al. 2014). Additionally, extraction methods influence the chemical composition of the extracts, making it essential to thoroughly characterize all-natural mixtures for experiment repeatability (Dhifi et al. 2016).

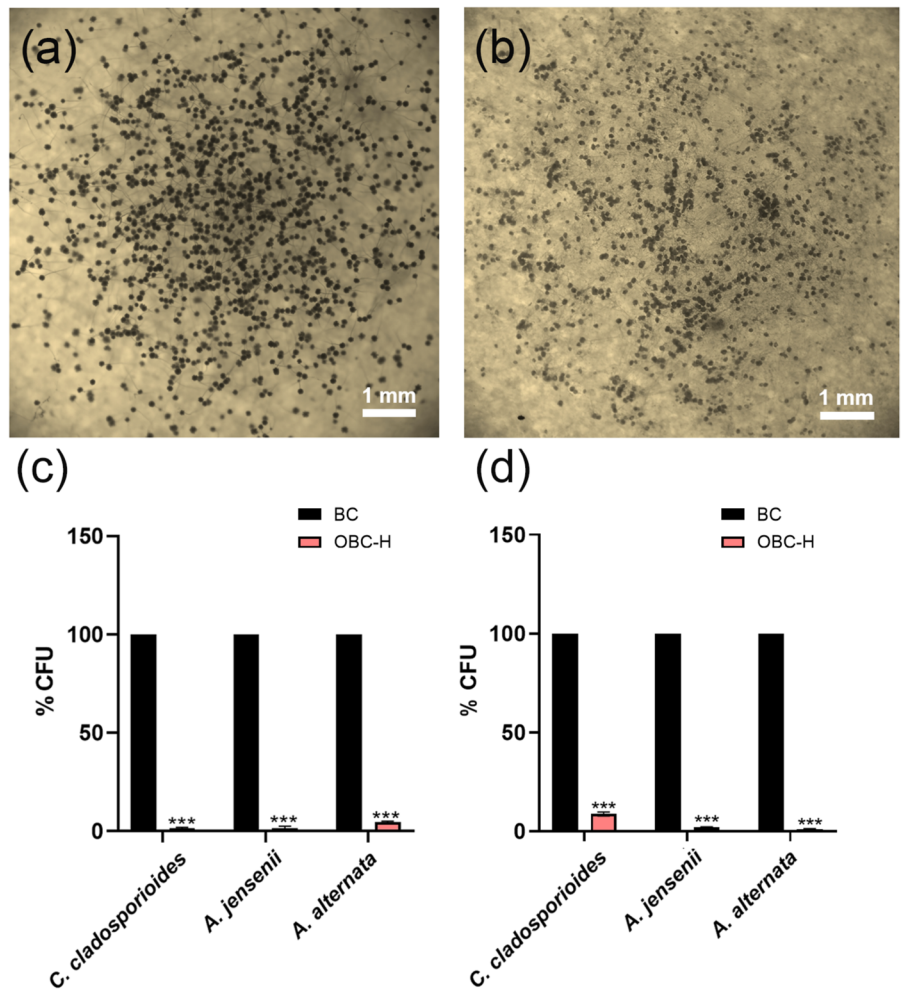

Fig. 10 Laboratory simulation experiment with *C. cladosporioides*, *A. jensenii* and *A. alternata* fungal strains. Micro-photographs obtained at the stereomicroscope of *A. alternata* mycelium grown on marble specimen surface before (**a**) and after (**b**) OBC-H hydrogel treatment. Fungal species viability following a 24-h treatment with OBC-H for marble (**c**) and biocalcarenitic stone (**d**) specimens, evaluated through CFU counting. Statistical analysis was conducted using a one-way ANOVA with the Bonferroni post-test (***$p < 0.001$ compared to untreated, denoted as control)

Evaluation of OBC hydrogel residues on treated stone and reusability

The potential presence of residual solvent or polymeric matter on cultural heritage surfaces after the treatment with gels generally raises concern. Indeed, the residues can impact the integrity and the appearance of treated materials, and they can be a source of degradation, particularly biodegradation (Domingues et al. 2013; Schifano et al. 2022).

In this study, the OBC hydrogels at all ozone concentrations have been easily peeled off by tweezers from the surface of the stone specimens, leaving no visible residues. To deep investigate the potential presence of cellulose residues on treated surfaces, a detailed analysis was conducted, as described in the materials and methods section, by μ-Raman spectroscopy on marble specimens (Fig. 11). After a 24-h treatment with OBC-H the Raman spectrum was collected (Fig. 11a) showing the only signals of calcite in the marble without the presence of cellulose signals (Fig. 11b). As already demonstrated for other self-standing peelable gels (Baglioni et al. 2021), the OBC-H hydrogel does not leave residues on treated surfaces.

It has also evaluated the possibility to use the OBC-H hydrogel twice. This was evaluated applying the hydrogel twice on marble specimens previously contaminated with *A. aurescens* for two hours each time. In the second cleaning, the sample exhibited at 100% antimicrobial activity (data not shown).

Conclusion

In conclusion, this study demonstrates the potential of ozonated bacterial cellulose (OBC) hydrogels as a green and effective antimicrobial solution to mitigate stone biodeterioration. The pristine bacterial cellulose (BC) hydrogel exhibited a nanofibrillar network with high purity and crystallinity and mechanical properties suitable for stone applications as a self-standing hydrogel. The ozonation of BC resulted in OBC hydrogels with varying ozone concentrations. The highest concentration, OBC-H, showed a complete suppression of bacterial and fungal spores' viability after 24 h treatment. The OBC-H hydrogel showed an effective loading of ozone-dissolved water, with slight modification of the BC chemical structure and water holding capacity (WHC) due to ozonation. When stored at 4 °C, a shelf-life of 30 days was assessed regarding antibacterial and antifungal spores' activity. Laboratory simulation experiments on different lithotypes demonstrated the remarkable antibacterial and

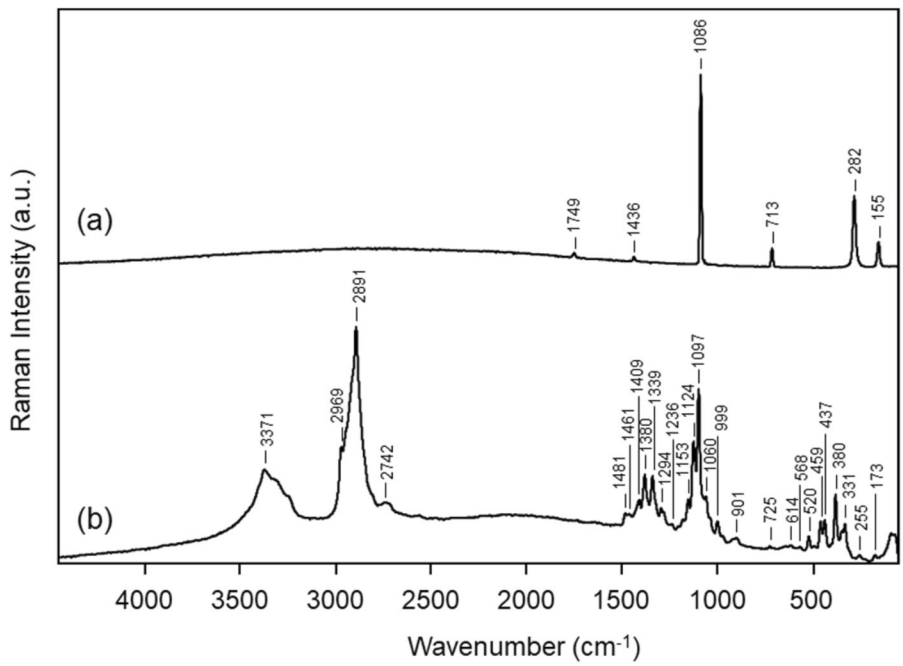

Fig. 11 Evaluation of OBC-H hydrogel residues on treated marble surfaces by μ-Raman spectroscopy. Raman spectra **a** collected after a 24-h treatment; reference spectrum **b** obtained from the dried OBC-H hydrogel

antifungal activities of OBC-H. Furthermore, OBC-H hydrogel could be easily peeled off after the treatment without leaving residues on stone surfaces. It also showed full antimicrobial efficacy in a subsequent re-application. This innovative material addresses the drawbacks associated with traditional biocides and synthetic polymers, offering a renewable, biodegradable, and easy-to-use solution for stone cleaning.

Acknowledgments The authors would like to thank Prof. Jacopo Tirillò and Prof. Fabrizio Sarasini for initial mechanical testing; Prof. Olga Russina for diffraction studies; Dr. Elisabetta Preziosi for the use of the spectrophotometer and Dr. Francesco Mura for electron microscopy analysis.

Author's contribution ES and ES contributed equally to this work. ES, ES, SA, MS, FM and AM contributed to methodology, investigation, and data curation. ES and ES contributed to original draft preparation. DU, LD, MLS and MSS contributed to supervision and writing-reviewing and editing. MLS contributed to project administration and funding acquisition. All authors read and approved the final manuscript.

Funding Open access funding provided by Università degli Studi di Roma La Sapienza within the CRUI-CARE Agreement. The research was funded by PNRR PE05-CHANGES-SPOKE 7. Protection and Conservation of Cultural Heritage against Climate Changes, Natural and Anthropic Risks. CUP B53C22003780006.

Data availability No datasets were generated or analysed during the current study.

Declarations

Conflict of interest The authors have no relevant financial or non-financial interests to disclose.

Ethical approval Not applicable.

References

Ahmed EM (2015) Hydrogel: Preparation, characterization, and applications: a review. J Adv Res 6:105–121. https://doi.org/10.1016/j.jare.2013.07.006

Atalla RH, VanderHart DL (1984) Native cellulose: a composite of two distinct crystalline forms. Science 223:283–285. https://doi.org/10.1126/science.223.4633.283

Baglioni M, Poggi G, Chelazzi D, Baglioni P (2021) Advanced materials in cultural heritage conservation. Molecules 26:3967. https://doi.org/10.3390/molecules26133967

Baglioni P, Baglioni M, Bonelli N, et al (2019) Smart soft nanomaterials for cleaning. In: Nanotechnologies and nanomaterials for diagnostic, conservation and restoration of cultural heritage. Elsevier, pp 171–204

Boccalon E, Nocchetti M, Pica M et al (2021) Hydrogels: A 'stepping stone' towards new cleaning strategies for biodeteriorated surfaces. J Cult Herit 47:1–11. https://doi.org/10.1016/j.culher.2020.07.008

Cai Z, Kim J (2010) Bacterial cellulose/poly(ethylene glycol) composite: characterization and first evaluation of biocompatibility. Cellulose 17:83–91. https://doi.org/10.1007/s10570-009-9362-5

Cappitelli F, Cattò C, Villa F (2020) The control of cultural heritage microbial deterioration. Microorganisms 8:1542. https://doi.org/10.3390/microorganisms8101542

Cappitelli F, Nosanchuk JD, Casadevall A et al (2007) Synthetic consolidants attacked by melanin-producing fungi: case study of the biodeterioration of Milan (Italy) cathedral marble treated with acrylics. Appl Environ Microbiol 73:271–277. https://doi.org/10.1128/AEM.02220-06

Carrillo-González R, Martínez-Gómez MA, MaDCA G-C, Mendoza Hernández JC (2016) Inhibition of microorganisms involved in deterioration of an archaeological site by silver nanoparticles produced by a green synthesis method. Sci Total Environ 565:872–881. https://doi.org/10.1016/j.scitotenv.2016.02.110

Caruso MR, D'Agostino G, Milioto S et al (2023) A review on biopolymer-based treatments for consolidation and surface protection of cultural heritage materials. J Mater Sci 58:12954–12975. https://doi.org/10.1007/s10853-023-08833-5

Chen H-H, Chen L-C, Huang H-C, Lin S-B (2011) In situ modification of bacterial cellulose nanostructure by adding CMC during the growth of Gluconacetobacter xylinus. Cellulose 18:1573–1583. https://doi.org/10.1007/s10570-011-9594-z

Chen S-Q, Lopez-Sanchez P, Wang D et al (2018) Mechanical properties of bacterial cellulose synthesised by diverse strains of the genus Komagataeibacter. Food Hydrocolloids 81:87–95. https://doi.org/10.1016/j.foodhyd.2018.02.031

Chirat C, Lachenal D (1994) Effect of ozone on pulp components. Appl Bleaching Kraft Pulps. 48:133–139. https://doi.org/10.1515/hfsg.1994.48.s1.133

Costa VLD, Costa AP, Amaral ME et al (2016) Effect of hot calendering on physical properties and water vapor transfer resistance of bacterial cellulose films. J Mater Sci 51:9562–9572. https://doi.org/10.1007/s10853-016-0112-4

Cutler NA, Oliver AE, Viles HA, Whiteley AS (2012) Non-destructive sampling of rock-dwelling microbial communities using sterile adhesive tape. J Microbiol Methods 91:391–398. https://doi.org/10.1016/j.mimet.2012.09.022

De France KJ, D'Emilio E, Cranston ED et al (2020) Dual physically and chemically crosslinked regenerated cellulose—Gelatin composite hydrogels towards art restoration. Carbohyd Polym 234:115885. https://doi.org/10.1016/j.carbpol.2020.115885

Dhifi W, Bellili S, Jazi S et al (2016) Essential oils' chemical characterization and investigation of some biological activities: a critical review. Medicines 3:25. https://doi.org/10.3390/medicines3040025

Domingues JAL, Bonelli N, Giorgi R et al (2013) Innovative hydrogels based on semi-interpenetrating p(HEMA)/PVP networks for the cleaning of water-sensitive cultural heritage artifacts. Langmuir 29:2746–2755. https://doi.org/10.1021/la3048664

Ettenauer JD, Jurado V, Piñar G et al (2014) Halophilic microorganisms are responsible for the rosy discolouration of saline environments in three historical buildings with mural paintings. PLoS ONE 9:e103844. https://doi.org/10.1371/journal.pone.0103844

Favero-Longo SE, Laurenzi Tabasso M, Brigadeci F et al (2022) A first assessment of the biocidal efficacy of plant essential oils against lichens on stone cultural heritage, and the importance of evaluating suitable application protocols. J Cult Herit 55:68–77. https://doi.org/10.1016/j.culher.2022.02.006

Fawcett TG, Crowder CE, Kabekkodu SN et al (2013) Reference materials for the study of polymorphism and crystallinity in cellulosics. Powder Diffr 28:18–31. https://doi.org/10.1017/S0885715612000930

Fidanza MR, Caneva G (2019) Natural biocides for the conservation of stone cultural heritage: a review. J Cult Herit 38:271–286. https://doi.org/10.1016/j.culher.2019.01.005

French AD (2014) Idealized powder diffraction patterns for cellulose polymorphs. Cellulose 21:885–896. https://doi.org/10.1007/s10570-013-0030-4

Gabriele F, Bruno L, Casieri C et al (2022) Application and monitoring of oxidative alginate-biocide hydrogels for two case studies in "The Sassi and the Park of the Rupestrian Churches of Matera." Coatings 12:462. https://doi.org/10.3390/coatings12040462

Gao X, Shi Z, Kuśmierczyk P et al (2016) Time-dependent rheological behaviour of bacterial cellulose hydrogel. Mater Sci Eng, C 58:153–159. https://doi.org/10.1016/j.msec.2015.08.019

Gaylarde C, Little B (2022) Biodeterioration of stone and metal—fundamental microbial cycling processes with spatial and temporal scale differences. Sci Total Environ 823:153193. https://doi.org/10.1016/j.scitotenv.2022.153193

Grazzini A, Fasana S, Zerbinatti M, Lacidogna G (2020) Non-destructive tests for damage evaluation of stone columns: the case study of Sacro Monte in Ghiffa (Italy). Appl Sci 10:2673. https://doi.org/10.3390/app10082673

Hu Y, Catchmark JM, Zhu Y et al (2014) Engineering of porous bacterial cellulose toward human fibroblasts ingrowth for tissue engineering. J Mater Res 29:2682–2693. https://doi.org/10.1557/jmr.2014.315

Kakakhel MA, Wu F, Gu J-D et al (2019) Controlling biodeterioration of cultural heritage objects with biocides: a review. Int Biodeterior Biodegradation 143:104721. https://doi.org/10.1016/j.ibiod.2019.104721

Lai C, Sheng L, Liao S et al (2013) Surface characterization of TEMPO-oxidized bacterial cellulose. Surf Interface Anal 45:1673–1679. https://doi.org/10.1002/sia.5306

Liu X, Koestler RJ, Warscheid T et al (2020) Microbial deterioration and sustainable conservation of stone monuments and buildings. Nat Sustain 3:991–1004. https://doi.org/10.1038/s41893-020-00602-5

Liu X, Meng H, Wang Y et al (2018) Water is a critical factor in evaluating and assessing microbial colonization and destruction of Angkor sandstone monuments. Int Biodeterior Biodegradation 133:9–16. https://doi.org/10.1016/j.ibiod.2018.05.011

Lo Schiavo S, De Leo F, Urzì C (2020) Present and future perspectives for biocides and antifouling products for stone-built cultural heritage: ionic liquids as a challenging alternative. Appl Sci 10:6568. https://doi.org/10.3390/app10186568

Mohammadkazemi F, Khademibarangenani R, Koosha M (2019) The effect of oxidation time and concentration on physicochemical, structural, and thermal properties of bacterial nano-cellulose. Polym Sci Ser A 61:265–273. https://doi.org/10.1134/S0965545X19030088

Negi A, Sarethy IP (2019) Microbial biodeterioration of cultural heritage: events, colonization, and analyses. Microb Ecol 78:1014–1029. https://doi.org/10.1007/s00248-019-01366-y

Nezhadali A, Nabavi M, Rajabian M et al (2014) Chemical variation of leaf essential oil at different stages of plant growth and in vitro antibacterial activity of Thymus vulgaris Lamiaceae, from Iran. Beni-Suef Univ J Basic Appl Sci 3:87–92. https://doi.org/10.1016/j.bjbas.2014.05.001

Numata Y, Kono H, Mori A et al (2019) Structural and rheological characterization of bacterial cellulose gels obtained from Gluconacetobacter genus. Food Hydrocoll 92:233–239. https://doi.org/10.1016/j.foodhyd.2019.01.060

Orlando I, Basnett P, Nigmatullin R et al (2020) Chemical modification of bacterial cellulose for the development of an antibacterial wound dressing. Front Bioeng Biotechnol 8:557885. https://doi.org/10.3389/fbioe.2020.557885

Pacelli S, Paolicelli P, Avitabile M et al (2018) Design of a tunable nanocomposite double network hydrogel based on gellan gum for drug delivery applications. Eur Polymer J 104:184–193. https://doi.org/10.1016/j.eurpolymj.2018.04.034

Palla F, Bruno M, Mercurio F et al (2020) Essential oils as natural biocides in conservation of cultural heritage. Molecules 25:730. https://doi.org/10.3390/molecules25030730

Paximada P, Dimitrakopoulou EA, Tsouko E et al (2016) Structural modification of bacterial cellulose fibrils under ultrasonic irradiation. Carbohyd Polym 150:5–12. https://doi.org/10.1016/j.carbpol.2016.04.125

Qi-Wang M-Y, He L-Y, Sheng X-F (2011) Characterization of bacterial community inhabiting the surfaces of weathered bricks of Nanjing Ming city walls. Sci Total Environ 409:756–762. https://doi.org/10.1016/j.scitotenv.2010.11.001

Ranaldi R, Rugnini L, Gabriele F et al (2022) Plant essential oils suspended into hydrogel: development of an easy-to-use protocol for the restoration of stone cultural heritage. Int Biodeterior Biodegradation 172:105436. https://doi.org/10.1016/j.ibiod.2022.105436

Romani M, Warscheid T, Nicole L et al (2022) Current and future chemical treatments to fight biodeterioration of outdoor building materials and associated biofilms: moving away from ecotoxic and towards efficient, sustainable solutions. Sci Total Environ 802:149846. https://doi.org/10.1016/j.scitotenv.2021.149846

Rugnini L, Migliore G, Tasso F et al (2020) Biocidal activity of phyto-derivative products used on phototrophic biofilms growing on stone surfaces of the Domus Aurea in Rome (Italy). Appl Sci 10:6584. https://doi.org/10.3390/app10186584

Salvatici T, Centauro I, Calandra S et al (2023) Non-destructive methods applied for in situ mechanical diagnosis: florentine historical buildings in Pietra Serena. Herit Sci 11:116. https://doi.org/10.1186/s40494-023-00959-8

Santo AP, Agostini B, Cuzman OA et al (2023) Essential oils to contrast biodeterioration of the external marble of Florence Cathedral. Sci Total Environ 877:162913. https://doi.org/10.1016/j.scitotenv.2023.162913

Schifano E, Cavallini D, De Bellis G et al (2020) Antibacterial effect of zinc oxide-based nanomaterials on environmental biodeteriogens affecting historical buildings. Nanomaterials 10:335. https://doi.org/10.3390/nano10020335

Schifano E, Conta G, Preziosi A et al (2022) 2-hydroxyisobutyric acid (2-HIBA) modulates ageing and fat deposition in Caenorhabditis elegans. Front Mol Biosci 9:986022. https://doi.org/10.3389/fmolb.2022.986022

Segal L, Creely JJ, Martin AE, Conrad CM (1959) An empirical method for estimating the degree of crystallinity of native cellulose using the x-ray diffractometer. Text Res J 29:786–794. https://doi.org/10.1177/004051755902901003

Skvortsova ZN, Gromovykh TI, Grachev VS, Traskin VYu (2019) Physicochemical mechanics of bacterial cellulose. Colloid J 81:366–376. https://doi.org/10.1134/S1061933X19040161

Takai M, Tsuta Y, Hayashi J, Watanabe S (1975) Biosynthesis of cellulose by acetobacter xylinum. III. X-ray studies of preferential orientation of the crystallites in a bacterial cellulose membrane. Polym J 7:157–164. https://doi.org/10.1295/polymj.7.157

Tescari M, Frangipani E, Caneva G et al (2018) Arthrobacter agilis and rosy discoloration in "Terme del Foro" (Pompeii, Italy). Int Biodeterior Biodegradation 130:48–54. https://doi.org/10.1016/j.ibiod.2018.03.015

Tripathi SK, Bhardwaj NK, Roy Ghatak H (2020) Developments in ozone-based bleaching of pulps. Ozone Sci Eng 42:194–210. https://doi.org/10.1080/01919512.2019.1647407

Trovão J, Portugal A, Soares F et al (2019) Fungal diversity and distribution across distinct biodeterioration phenomena in limestone walls of the old cathedral of Coimbra, UNESCO World Heritage Site. Int Biodeterior Biodegradation 142:91–102. https://doi.org/10.1016/j.ibiod.2019.05.008

Tsouko E, Kourmentza C, Ladakis D et al (2015) Bacterial cellulose production from industrial waste and by-product streams. IJMS 16:14832–14849. https://doi.org/10.3390/ijms160714832

Ul-Islam M, Khan T, Park JK (2012) Water holding and release properties of bacterial cellulose obtained by in situ and ex situ modification. Carbohyd Polym 88:596–603. https://doi.org/10.1016/j.carbpol.2012.01.006

Vasconcelos NF, Andrade FK, Vieira LDAP et al (2020) Oxidized bacterial cellulose membrane as support for enzyme immobilization: properties and morphological features. Cellulose 27:3055–3083. https://doi.org/10.1007/s10570-020-02966-5

Vasconcelos NF, Feitosa JPA, Da Gama FMP et al (2017) Bacterial cellulose nanocrystals produced under different hydrolysis conditions: Properties and morphological features. Carbohyd Polym 155:425–431. https://doi.org/10.1016/j.carbpol.2016.08.090

Wada M, Okano T (2001) No title found. Cellulose 8:183–188. https://doi.org/10.1023/A:1013196220602

Warscheid Th, Braams J (2000) Biodeterioration of stone: a review. Int Biodeterior Biodegradation 46:343–368. https://doi.org/10.1016/S0964-8305(00)00109-8

Yang KY, Wloch D, Lee K-Y (2021) TEMPO-oxidised nanocellulose hydrogels and self-standing films derived from bacterial cellulose nanopaper. RSC Adv 11:28352–28360. https://doi.org/10.1039/D1RA04190H

Zhang G, Gong C, Gu J et al (2019) Biochemical reactions and mechanisms involved in the biodeterioration of stone world cultural heritage under the tropical climate conditions. Int Biodeterior Biodegradation 143:104723. https://doi.org/10.1016/j.ibiod.2019.104723